

Communication: Observation of local-bender eigenstates in acetylene

Adam H. Steeves, G. Barratt Park, Hans A. Bechtel, Joshua H. Baraban, and Robert W. Field

Citation: *The Journal of Chemical Physics* **143**, 071101 (2015); doi: 10.1063/1.4928638View online: <http://dx.doi.org/10.1063/1.4928638>View Table of Contents: <http://scitation.aip.org/content/aip/journal/jcp/143/7?ver=pdfcov>

Published by the AIP Publishing

Articles you may be interested in[Experimental observation and analysis of the 3v1\(\$\Sigma_g\$ \) stretching vibrational state of acetylene using continuous-wave infrared stimulated emission](#)*J. Chem. Phys.* **139**, 054201 (2013); 10.1063/1.4816524[High resolution study of spin-orbit mixing and the singlet-triplet gap in chlorocarbene: Stimulated emission pumping spectroscopy of CH 35 Cl and CD 35 Cl](#)*J. Chem. Phys.* **129**, 104309 (2008); 10.1063/1.2977686[Discovery of the optically forbidden S 1 –S 0 transition of silylidene \(H 2 C = Si \)](#)*J. Chem. Phys.* **118**, 1642 (2003); 10.1063/1.1531618[The vibrational energy pattern in acetylene \(IV\): Updated global vibration constants for 12 C 2 H 2](#)*J. Chem. Phys.* **110**, 2074 (1999); 10.1063/1.477817[Structurally mixed molecular eigenstates of 2-fluoroethanol resulting from conformational isomerization](#)*J. Chem. Phys.* **107**, 8189 (1997); 10.1063/1.475119



NEW Special Topic Sections

NOW ONLINE
Lithium Niobate Properties and Applications:
Reviews of Emerging Trends

AIP Applied Physics
Reviews

Communication: Observation of local-bender eigenstates in acetylene

Adam H. Steeves,^{1,2} G. Barratt Park,^{1,3} Hans A. Bechtel,^{1,4} Joshua H. Baraban,^{1,5} and Robert W. Field^{1,a)}

¹Department of Chemistry, Massachusetts Institute of Technology, Cambridge, Massachusetts 02139, USA

²Department of Chemistry and Biochemistry, Ithaca College, Ithaca, New York 14850, USA

³Max Planck Institute for Biophysical Chemistry, Göttingen, Germany

⁴Advanced Light Source, Lawrence Berkeley National Laboratory, Berkeley, California 94720, USA

⁵Department of Chemistry and Biochemistry, University of Colorado, Boulder, Colorado 80309, USA

(Received 6 July 2015; accepted 4 August 2015; published online 19 August 2015)

We report the observation of eigenstates that embody large-amplitude, local-bending vibrational motion in acetylene by stimulated emission pumping spectroscopy via vibrational levels of the S_1 state involving excitation in the non-totally symmetric bending modes. The $N_b = 14$ level, lying at 8971.69 cm^{-1} ($J = 0$), is assigned on the basis of degeneracy due to dynamical symmetry breaking in the local-mode limit. The level pattern for the $N_b = 16$ level, lying at 10218.9 cm^{-1} , is consistent with expectations for increased separation of $\ell = 0$ and 2 vibrational angular momentum components. Increasingly poor agreement between our observations and the predicted positions of these levels highlights the failure of currently available normal mode effective Hamiltonian models to extrapolate to regions of the potential energy surface involving large-amplitude displacement along the acetylene \rightleftharpoons vinylidene isomerization coordinate. © 2015 AIP Publishing LLC. [<http://dx.doi.org/10.1063/1.4928638>]

Local-mode models of molecular vibrations are appealing because they provide a reduced-dimension picture in which the observed transition frequencies can be directly connected to the forces required to distort a molecule along chemically intuitive coordinates. In fact, these local-modes are not only intuitive but also physically appropriate for many highly vibrationally excited systems, where the diagonal anharmonicity associated with an isolated bond oscillator overwhelms the potential- and kinetic-energy coupling terms connecting symmetrically related oscillators.¹ As a result, local mode models have demonstrated significant utility in the interpretation of X–H stretching spectra approaching the X–H dissociation limit.²

Large amplitude local-bending vibrational motions have been predicted to exist on the acetylene S_0 surface by a number of methods.^{3–9} If these states could be experimentally observed, they would serve as exquisite probes of the acetylene \rightleftharpoons vinylidene isomerization path. The acetylene vibrational levels most strongly affected by the presence of the vinylidene isomeric minimum will be those that are spatially localized near the isomerization barrier separating the acetylene and vinylidene regions of the potential energy surface.

Despite the importance of the local-bending states, experimental observation has been hindered by lack of spectroscopic access, dictated by selection rules associated with overtone-pumping and stimulated emission pumping (SEP) experiments.¹⁰ In an SEP experiment, the change in geometry between the ground and excited (intermediate) electronic states determines the dynamics sampled in the spectrum. As the S_1 state of acetylene is *trans*-bent ($\angle\text{CCH} = 122.5^\circ$) with an elongated C–C bond ($r_{\text{CC}} = 1.375\text{ Å}$) at its equilibrium geometry,¹¹

large amplitude *trans*-bending dynamics are sampled in the SEP spectrum recorded from this intermediate state. That is, in SEP spectra from S_1 Franck-Condon active levels, the zero-order bright states have excitation in the *trans*-bending mode (ν_4'', π_g) and to a lesser extent the C–C stretching mode (ν_2'', σ_g^+).

The normal-to-local transition is calculated to occur in the range of $N_b = 10$ –14,¹² where $N_b = \nu_4'' + \nu_5''$ denotes the total quanta of bend excitation. Over this range, the lowest member of a polyad shifts from primarily *trans*-bending in character to primarily local-bending. This shift coincides with a decrease of the intensity of the lowest polyad member, as observed from a Franck-Condon active vibrational level of S_1 . The lowest members of the $N_b = 10$ and 12 polyads were easily observed in previous dispersed fluorescence (DF) experiments,¹³ while the lowest member of the $N_b = 14$ polyad was too weak to be observed in these spectra. The $N_b = 14$ level is the lowest-energy level believed to possess primarily local-mode character, and therefore its observation is crucial to the understanding of the normal-to-local transition.

In order to sidestep the limited spectroscopic access provided by the Franck-Condon active vibrational levels, we have reinvestigated the $\tilde{A} \leftarrow \tilde{X}$ spectrum of acetylene with a focus on the non-totally symmetric vibrational modes.^{14–20} This work has enabled us to perform a detailed calculation of the Franck-Condon factors^{21,22} and to develop a model that successfully describes the Franck-Condon fluorescence propensities from the non-totally symmetric modes of the S_1 state.²³ The model takes into account anharmonic interactions and correctly reproduces the observed emission patterns from B^1 and B^2 polyads. (The notation B^n denotes an S_1 bending polyad with $\nu_4' + \nu_6' = n$.) The results indicate that the zero-order ν_6' (in-plane *cis* bend) vibration excites the ν_5' *cis* bend with the correct relative phase to provide

^{a)}Electronic mail: rwfield@mit.edu

intensity into zero-order local bender states, in keeping with semiclassical arguments. This motivated us to employ the lowest energy member of B^n overtone polyads (denoted B^n , I) as SEP intermediates, because these levels have the largest fractional character of ν'_6 . Although the crucial $N_b = 14$ state has not previously been observed, the spectroscopic effective Hamiltonian that describes all of the observed vibrational data provides useful predictions of the $N_b = 14$ local-bender state. Using the 3^1B^4 , I ($K = 1$) level¹⁶ as an intermediate, strong SEP signals were observed around the predicted position of the lowest-energy local-bender state. Spectra were recorded from a number of rotational levels in order to establish the rotational assignments of the lower state (Fig. 1). These measurements identify a $\Sigma_g^+(\ell = 0)$ state, at an energy ($J = 0$) of 8971.69 cm^{-1} , as well as its corresponding $\Delta_g(\ell = 2)$ state. A complete prediction of the energy levels in this region²⁴ gives four expected Σ_g^+ states in the energy region of $8960\text{--}8990\text{ cm}^{-1}$, with the local-bender state predicted at the top end of this range, 8983 cm^{-1} .

Because the prediction²⁴ of the local-bending energy is over 10 cm^{-1} higher than our observed state, one critical observation is required to verify the assignment of the $N_b = 14$ local-bending level. This observation is related to the systematic degeneracy that is a hallmark of local mode behavior. Of the Σ_g^+ states predicted in this energy region, the only one predicted to be degenerate with a Σ_u^+ level is the local-bender. IR-UV dispersed fluorescence has identified a level with Σ_u^+ symmetry at 8971.76 cm^{-1} ,²⁵ however, the authors of that work did not comment on the local-mode character of this state. Through these complementary experiments, two states are observed that are degenerate (within the experimental uncertainty) but possess opposite g/u symmetry. On this basis, these states can be assigned conclusively as the $N_b = 14$ local-bender pair.

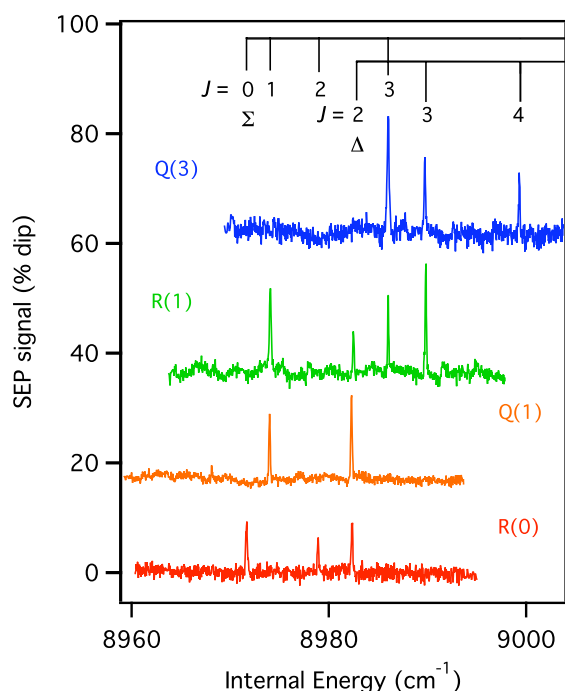


FIG. 1. SEP spectra of the $N_b = 14$ local-bender state recorded from 3^1B^4 , I . Spectra are recorded from several rotational levels of the intermediate in order to label the lower-state J values.

We have searched for the local-bend state in the $N_b = 16$ polyad using the same intermediate state as was used to observe the $N_b = 14$ local-bender state. The region $10\,200\text{--}10\,250\text{ cm}^{-1}$ was searched by SEP, but only very weak features were located and these could not be assembled into meaningful rotational band structure. Unfortunately, this indicates that the 3^1B^4 , I state cannot serve as a universal gateway into all of the local-bender levels. We have performed a Franck-Condon calculation in the harmonic basis, which predicts that the access to local-bender levels from 3^1B^4 reaches a maximum at $N_b = 12\text{--}14$ and falls off in the $N_b = 16\text{--}18$ range. (The results of the Franck-Condon calculation are shown in the supplementary material.²⁶) Our calculation indicates that an alternative intermediate state, B^4 , I , achieves peak local-bender access at higher bending quanta ($N_b = 14\text{--}16$). We searched for the $N_b = 16$ local bender eigenstate via SEP from this intermediate as well. The spectra contained many of the weak features found in SEP from 3^1B^4 , indicating that they are real SEP features and not upward-going double resonance transitions. In addition, a new band is observed at an energy ($J = 0$) of $10\,218.9\text{ cm}^{-1}$. Clear branch structure is found in SEP spectra from multiple rotational levels of the intermediate state. Transitions into the lowest rotational levels of this state are shown in Fig. 2(d).

Unfortunately, the information available for the *ungerade* manifold does not include the lowest-energy states of pure-bending polyads above $N_b = 14$, so that a definitive assignment cannot be made on the basis of systematic degeneracies. The local bender energies predicted by two polyad models^{24,25} are compared with our direct experimental observations in Table I. The fit model of Ref. 24 does not include any pure-bend polyads above $N_b = 12$, whereas the fit model of Ref. 25 includes data from both *gerade* and *ungerade* polyads up to $N_b = 14$, and therefore samples bending energies where local mode emergence occurs. The predictions of Ref. 25 are in much closer agreement with experiment. In particular, the results of Ref. 25 correctly predict the approximate splitting between the g/u local bender pairs as a function of N_b , whereas Ref. 24 predicts that the degeneracy between g/u pairs emerges at too low an energy. However, both models appear to predict systematically too high energies for the local-bending states, and the discrepancy is expected to increase further for the higher energy states. Even the results of Ref. 25, which are fitted to data that include the *ungerade* $N_b = 14$ local bender, give this state as an outlier with a residual of over 3 cm^{-1} .²⁵ It is known that in the vicinity of an isomerization barrier (where the classical vibrational frequency approaches zero), the vibrational progressions along modes that sample the isomerization coordinate are poorly reproduced by low-order Dunham-type expansions,²⁷ whereas models that specifically allow for a Dixon-type frequency dip²⁸ efficiently reproduce the level structure.²⁹ We therefore expect the effective local-bending frequency to be increasingly poorly predicted by the available fit models as the energy approaches the acetylene \rightleftharpoons vinylidene barrier ($\sim 15\,200\text{ cm}^{-1}$), with the observed levels falling further and further below the model predictions. For this reason, we are unlikely to be able to assign higher-lying local bender levels solely on extrapolation of the currently available polyad models.

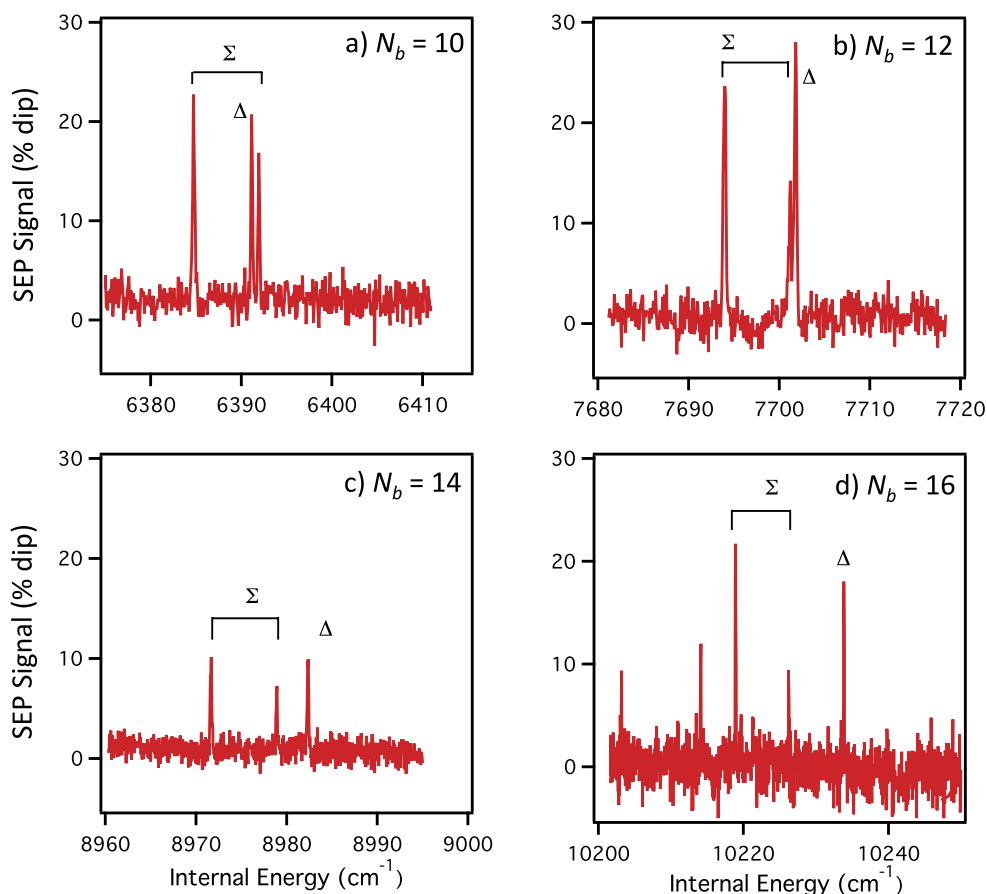


FIG. 2. SEP spectra of the lowest members of the $N_b = 10$ –16 polyads. Transitions into the $N_b = 10$ and 12 polyads are recorded from Franck–Condon-active intermediate levels (using R(0) PUMP transitions). Transitions into the $N_b = 14$ and 16 polyads use Franck–Condon-forbidden levels as intermediates: the spectra of $N_b = 14$ are recorded from 3^1B^4 , I , and those for $N_b = 16$ are recorded from B^4 , I . The pattern of the Σ/Δ splittings suggests that the state observed at $10\,218.9\text{ cm}^{-1}$ is the $N_b = 16$ local-bender Σ state.

Amano *et al.*³⁰ have proposed another spectroscopic fit model based on an expansion of the linear molecule Hamiltonian, which directly incorporates the vibrational angular momentum structure. The authors of that work have reported data up to $N_b = 12$, with excellent agreement, but it is not immediately clear that such a model will extrapolate well into the local-mode regime, since it is constructed from normal mode basis

states and was not designed to behave correctly in the vicinity of the isomerization. Alternatively, the data may be fitted to a Hamiltonian expressed in the local-mode basis.^{12,31} It may be easier to address problems with local-mode anharmonicity in such a treatment, but since so few local-bending states have been observed, the model will need to be parameterized to the energies of the low energy normal-mode states.

Without an accurate fit prediction or an observation of the degenerate *ungerade* pair, it is difficult to make a definitive vibrational assignment of the $N_b = 16$ local bender state. However, of the Σ_g^+ , Δ_g level pairs predicted within 50 cm^{-1} , most can be ruled out on the basis of Franck–Condon factors (levels with more than one quantum of ν_1'' or ν_3'' are expected to be too weak to observe), or on the basis of level patterns (levels with odd quanta of ν_3'' (σ_u^+) are expected to give rise to more than one Δ_g component). Other levels can be ruled out on the basis of the predicted splitting between the $\Sigma(\ell = 0)$ and $\Delta(\ell = 2)$ components. The magnitude of the splitting between the $\Sigma(\ell = 0)$ and $\Delta(\ell = 2)$ components of the lowest member of each *gerade* pure bending polyad increases regularly for the series $N_b = 10, 12, 14$ as the bending structure makes the transition from being well-described in the normal-mode basis to being well-described in the local-mode basis (Figs. 2 and 3). The large splitting can be rationalized in the local-mode limit as the molecule approaches the isomerization barrier. For a state with two quanta of vibrational angular momentum, some

TABLE I. The energy (in cm^{-1}) of the lowest member of each $J = \ell = 0$ pure bending polyad of $^{12}\text{C}_2\text{H}_2$, tabulated according to N_b and g/u symmetry.

N_b	Symmetry	Fit predictions ^a		Expt. ^c
		Reference 24	Reference 25 ^b	
10	Σ_g^+	6 386.55	6 383.04	6 384.74
10	Σ_u^+	6 395.96	6 394.53	6 395.30
12	Σ_g^+	7 697.66	7 693.92	7 694.27
12	Σ_u^+	7 697.64	7 694.23	7 694.74
14	Σ_g^+	8 982.66	8 974.76	8 971.69
14	Σ_u^+	8 982.66	8 974.76	8 971.76
16	Σ_g^+	10 247.22	10 229.93	10 218.9 ^d
16	Σ_u^+	10 247.22	10 229.93	

^aPredictions obtained from published fits to a polyad model.

^bPure bend fit, Table II of Ref. 25.

^cObserved *gerade* levels are from high-resolution SEP experiments in our lab, and *ungerade* levels are from the IR-UV dispersed fluorescence experiments of Ref. 25.

^dTentative assignment.

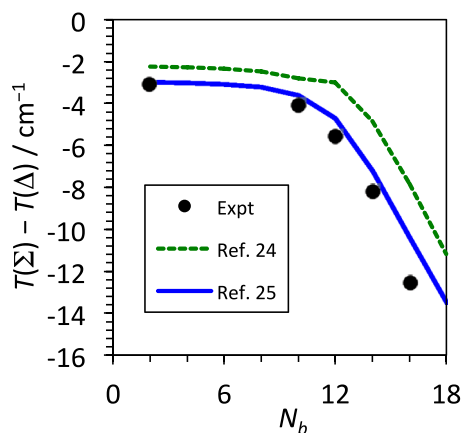


FIG. 3. The energy difference between the lowest member of each pure-bending Σ_g^+ and Δ_g polyad is plotted as a function of N_b . The trivial $B[J(J+1)-\ell^2]$ rotational energy has been subtracted from the Δ_g term values. The experimentally determined point at $N_b=2$ is from Ref. 33. Curves through the data are from the H_{eff} predictions of Refs. 24 and 25.

of the kinetic energy is directed perpendicular to the in-plane bending coordinate. This energy is “wasted” from the point of view of the isomerization reaction, so the wavefunction cannot explore the identical range of bending angle as the Σ state. As a result, the Δ state falls in energy less rapidly in response to softening of the potential along the local-bending coordinate. A similar ℓ -dependence has been noted in the HCP system,²⁷ and for HCN/HNC,³² but to our knowledge, our work provides the first demonstration of isomerization-induced ℓ -dependent mode softening in a tetra-atomic system. In the normal-mode basis of acetylene, the values of the splitting are associated with the diagonal terms in the effective Hamiltonian arising from the vibrational angular momentum associated with degenerate vibrational modes ($g_{ij}l_i l_j$). While the value g_{44} associated with the Franck-Condon active *trans*-bending mode ν_4'' is very small, the values of g_{45} and g_{55} are significant and positive.²⁵ Thus, in the normal mode picture, the increasing $\ell = 0-2$ splitting reflects the increasing admixture of *cis*-bending character for the lowest members of the $N_b = 10-16$ polyads. The $\Sigma - \Delta$ separation provides evidence that the state at $10\,218.9\text{ cm}^{-1}$ is the next member of the local-bender progression, though this assignment should be treated as tentative until the degenerate *ungerade* local bending partner is detected. We note that the observed position is almost 30 cm^{-1} lower than the energy predicted by one of the commonly used spectroscopic effective Hamiltonians (Table I).²⁴

Fortunately, our recent explorations of the S_1 state have provided a number of potential alternative intermediate states for future IR-UV-DF or IR-UV-SEP experiments that will continue to push assignments of the *ungerade* levels to higher energy. In particular, the members of B^3 and B^5 S_1 polyads^{14,18} will allow access to the missing member of the local-mode pair for $N_b = 16$ and higher. Ultimately, confirmation of the local-mode vibrational character of the states approaching the isomerization barrier will be provided by measurement of the

uniquely large electric dipole moments of these states.³⁴ Direct observations of large-amplitude local bending eigenstates in acetylene will enable a more accurate determination of the shape of the PES along the acetylene \rightleftharpoons vinylidene isomerization coordinate and may allow researchers to develop more accurate models that account directly for isomerization.

We are grateful to Annelise Beck for her assistance. This material is based upon work supported by the U.S. Department of Energy, Office of Science, Chemical Sciences Geosciences and Biosciences Division of the Basic Energy Sciences Office, under Award No. DE-FG0287ER13671.

- ¹M. S. Child and L. Halonen, *Adv. Chem. Phys.* **57**, 1–58 (1984).
- ²J. L. Fry, J. Matthews, J. R. Lane, C. M. Roehl, A. Sinha, H. G. Kjaergaard, and P. O. Wennberg, *J. Phys. Chem. A* **110**, 7072–7079 (2006).
- ³A. B. McCoy and E. L. Sibert, *J. Chem. Phys.* **105**, 459–468 (1996).
- ⁴E. L. Sibert and A. B. McCoy, *J. Chem. Phys.* **105**, 469–478 (1996).
- ⁵J. P. Rose and M. E. Kellman, *J. Chem. Phys.* **105**, 10743–10754 (1996).
- ⁶D. G. Xu, R. Q. Chen, and H. Guo, *J. Chem. Phys.* **118**, 7273–7282 (2003).
- ⁷R. Prossimi and S. C. Farantos, *J. Chem. Phys.* **118**, 8275–8280 (2003).
- ⁸V. Tyng and M. E. Kellman, *J. Phys. Chem. B* **110**, 18859–18871 (2006).
- ⁹H. Han, A. Li, and H. Guo, *J. Chem. Phys.* **141**, 244312 (2014).
- ¹⁰M. Silva, R. Jongma, R. W. Field, and A. M. Wodtke, *Annu. Rev. Phys. Chem.* **52**, 811–852 (2001).
- ¹¹T. R. Huet, M. Godefroid, and M. Herman, *J. Mol. Spectrosc.* **144**, 32–44 (1990).
- ¹²M. P. Jacobson, R. J. Silbey, and R. W. Field, *J. Chem. Phys.* **110**, 845–859 (1999).
- ¹³J. P. O’Brien, M. P. Jacobson, J. J. Sokol, S. L. Coy, and R. W. Field, *J. Chem. Phys.* **108**, 7100–7113 (1998).
- ¹⁴A. J. Merer, N. Yamakita, S. Tsuchiya, A. H. Steeves, H. A. Bechtel, and R. W. Field, *J. Chem. Phys.* **129**, 054304 (2008).
- ¹⁵A. H. Steeves, A. J. Merer, H. A. Bechtel, A. R. Beck, and R. W. Field, *Mol. Phys.* **106**, 1867–1877 (2008).
- ¹⁶A. H. Steeves, H. A. Bechtel, A. J. Merer, N. Yamakita, S. Tsuchiya, and R. W. Field, *J. Mol. Spectrosc.* **256**, 256–278 (2009).
- ¹⁷A. J. Merer, A. H. Steeves, J. H. Baraban, H. A. Bechtel, and R. W. Field, *J. Chem. Phys.* **134**, 244310 (2011).
- ¹⁸J. H. Baraban, P. B. Changala, A. J. Merer, A. H. Steeves, H. A. Bechtel, and R. W. Field, *Mol. Phys.* **110**, 2707–2723 (2012).
- ¹⁹J. H. Baraban, A. J. Merer, J. F. Stanton, and R. W. Field, *Mol. Phys.* **110**, 2725–2733 (2012).
- ²⁰J. Jiang, J. H. Baraban, G. B. Park, M. L. Clark, and R. W. Field, *J. Phys. Chem. A* **117**, 13696–13703 (2013).
- ²¹G. B. Park, *J. Chem. Phys.* **141**, 134304 (2014).
- ²²G. B. Park, J. H. Baraban, and R. W. Field, *J. Chem. Phys.* **141**, 134305 (2014).
- ²³G. B. Park, A. H. Steeves, J. H. Baraban, and R. W. Field, *J. Phys. Chem. A* **119**, 857–865 (2015).
- ²⁴M. Herman, A. Campargue, M. El Idrissi, and J. Vander Auwera, *J. Phys. Chem. Ref. Data* **32**, 921–1361 (2003).
- ²⁵K. Hoshina, A. Iwasaki, K. Yamanouchi, M. P. Jacobson, and R. W. Field, *J. Chem. Phys.* **114**, 7424–7442 (2001).
- ²⁶See supplementary material at <http://dx.doi.org/10.1063/1.4928638> for calculated vibronic intensity factors from the SEP intermediate levels used in this work.
- ²⁷M. P. Jacobson and M. S. Child, *J. Chem. Phys.* **114**, 262–275 (2001).
- ²⁸R. N. Dixon, *Trans. Faraday Soc.* **60**, 1363–1368 (1964).
- ²⁹J. H. Baraban, “Spectroscopic signatures of isomerization,” Ph.D. thesis, Massachusetts Institute of Technology, Cambridge, MA, 2013.
- ³⁰T. Amano, T. Sako, K. Hoshina, and K. Yamanouchi, *Chem. Phys. Lett.* **375**, 576–582 (2003).
- ³¹K. K. Lehmann, *J. Chem. Phys.* **96**, 8117–8119 (1992).
- ³²G. C. Mellau, *J. Chem. Phys.* **134**, 234303 (2011).
- ³³J. Plíva, *J. Mol. Spectrosc.* **44**, 165–182 (1972).
- ³⁴B. M. Wong, A. H. Steeves, and R. W. Field, *J. Phys. Chem. B* **110**, 18912–18920 (2006).